Electronic Supplementary Material (ESI) for Journal of Materials Chemistry A.


# Synergistic Effect of Diatomic Boron-doped Layered Two-Dimensional $MSi_2N_4$ Monolayer for Efficient Electrochemical Nitrogen Reduction

Qian Dang,[a] Yuqin Zhang ,[a] Xiaohang Wang,[a] Tianyong Liu,[a] Mingjie Zhang,*[a] Xingxing Li,[a] Shaobin Tang,*[a] and Jun Jiang[b]

[a]Key Laboratory of Organo-Pharmaceutical Chemistry of Jiangxi Province, Gannan Normal University, Ganzhou 341000, China

[b]Hefei National Laboratory for Physical Sciences at the Microscale, CAS Center for Excellence in Nanoscience, School of Chemistry and Materials Science, University of Science and Technology of China, Hefei 230026, China

**Table S1**. Gibbs free energy of potential-determining step ($\Delta G_{PDS}$, in eV) for NRR on B@$MoSi_2N_4$ with different supercell size by enzymatic pathway.

| | 3×1×3 | 4×1×4 | 5×1×5 |
|---|---|---|---|
| $\Delta G_{PDS}$ | 1.325 | 1.374 | 1.340 |

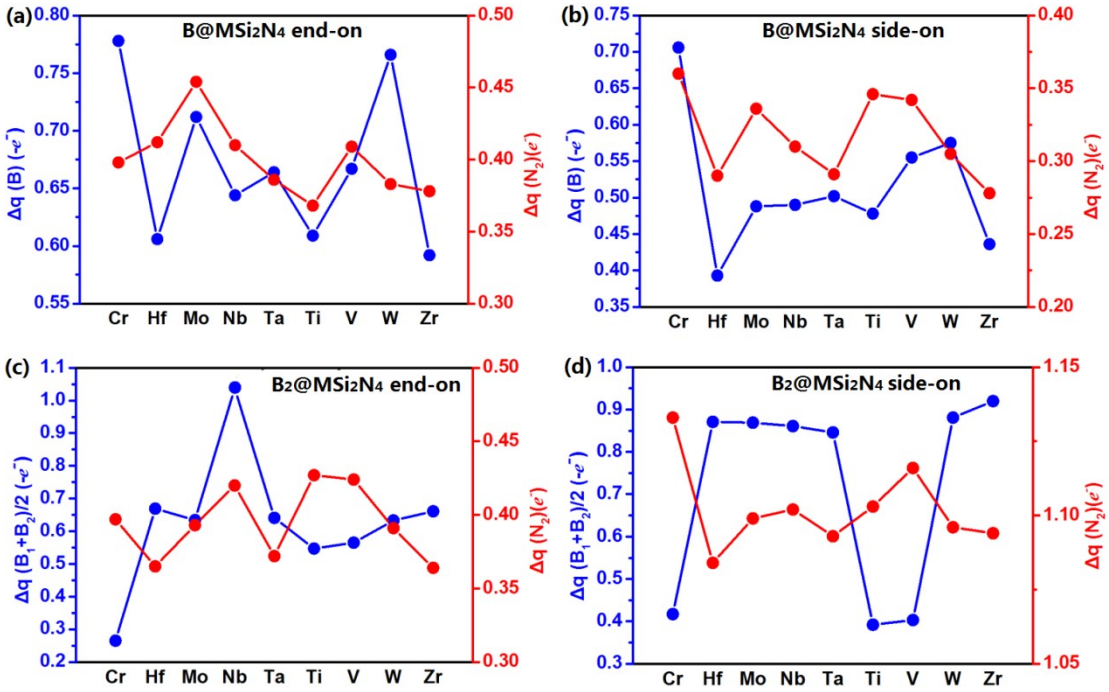


**Fig. S1** Positively polarized charges of per B atom and negatively polarized charges of $N_2$ for $N_2$ adsorbed on (a, b) B@$MSi_2N_4$ and (c, d) $B_2$@$MSi_2N_4$ with the (a, c) end-on and (b, d) side-on configurations.

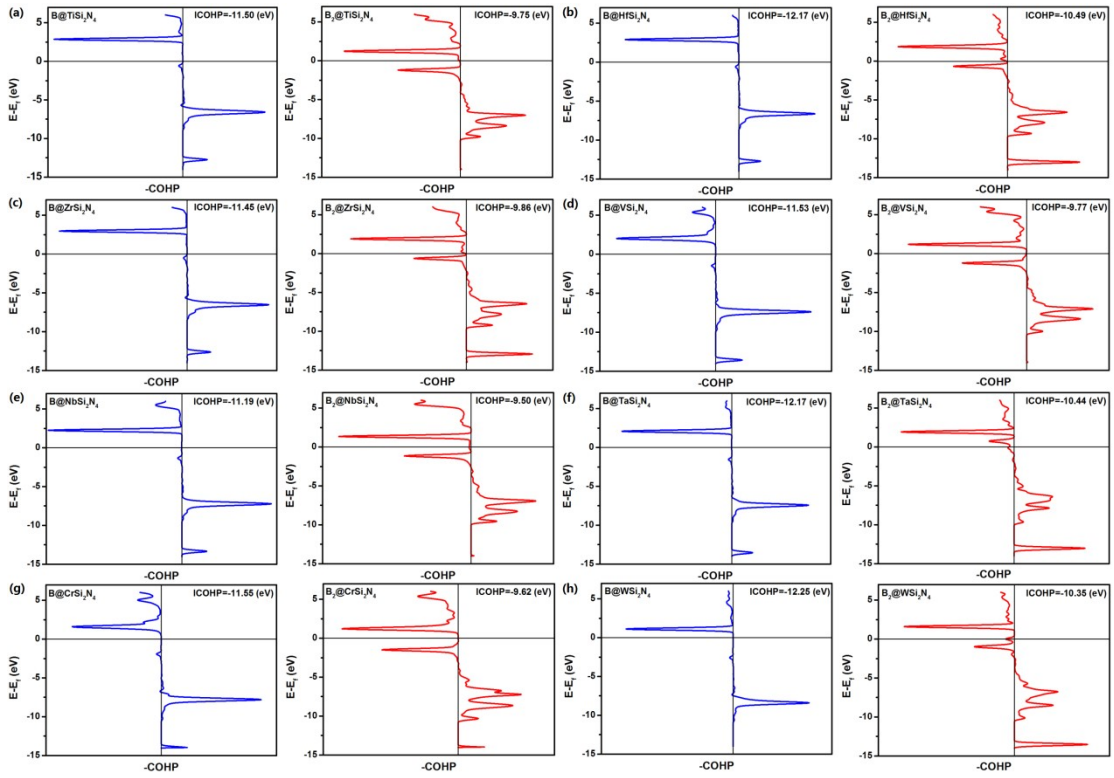


**Fig. S2** Crystal orbital Hamilton population of adsorbed $N_2$ on B@$MSi_2N_4$ (left panel) and $B_2$@$MSi_2N_4$ (right panel) with the end-on pattern (M=Ti, Hf, Zr, V, Nb, Ta, Cr, W). (a) Ti, (b) Hf, (c) Zr, (d) V, (e) Nb, (f) Ta, (g) Cr, and (h) W. ICOHP values for each system are shown. The Fermi level is set to 0.

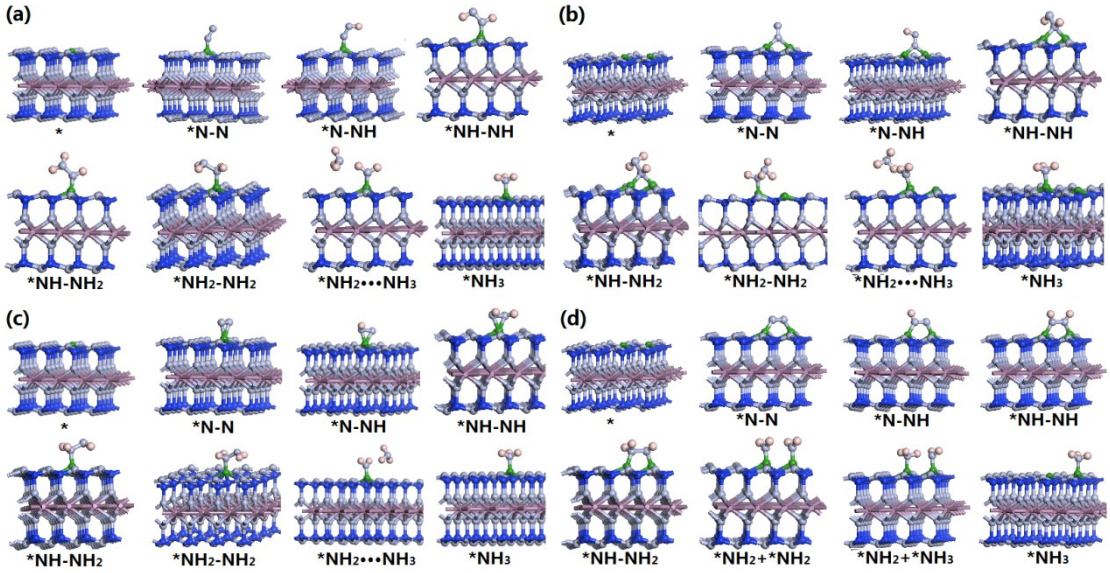


**Fig. S3** Geometrical structures of intermediates via (a) and (b) the alternating and (c) and (d) enzymatic reaction pathway on (a, c) one B and (b, d) two B atoms doped $MoSi_2N_4$.

**Table S2.** Adsorption energy (in eV) of key intermediates *N-N, *N-NH, *N-$NH_2$, *N-$NH_3$, *NH, *$NH_2$, and *$NH_3$ on B@$MSi_2N_4$ for eNRR via the distal mechanism.

| M | $\Delta E_{ads}$ (*N-N) | $\Delta E_{ads}$ (*N-NH) | $\Delta E_{ads}$ (*N-$NH_2$) | $\Delta E_{ads}$ (*N-$NH_3$) | $\Delta E_{ads}$ (*NH) | $\Delta E_{ads}$ (*$NH_2$) | $\Delta E_{ads}$ (*$NH_3$) |
|---|---|---|---|---|---|---|---|
| **Cr** | -2.26 | -1.04 | -2.12 | -1.65 | -0.76 | -2.93 | -4.20 |
| **Hf** | -1.84 | -0.58 | -1.61 | -1.03 | -0.14 | -2.39 | -3.76 |
| **Mo** | -1.97 | -0.66 | -1.75 | -1.17 | -0.35 | -2.56 | -3.89 |
| **Nb** | -1.90 | -0.87 | -1.69 | -1.23 | -0.48 | -2.51 | -3.83 |
| **Ta** | -1.86 | -0.66 | -1.64 | -1.10 | -0.33 | -2.48 | -3.80 |
| **Ti** | -2.07 | -0.80 | -1.87 | -1.33 | -0.54 | -2.68 | -4.01 |
| **V** | -2.13 | -0.91 | -1.94 | -1.39 | -0.58 | -2.78 | -4.07 |
| **W** | -2.00 | -0.75 | -1.79 | -1.31 | -0.43 | -2.65 | -3.93 |
| **Zr** | -1.80 | -0.46 | -1.59 | -1.02 | -0.24 | -2.37 | -3.74 |

* The adsorption energy of intermediate is calculated by the following equation:

$\Delta E_{ads} * N_X H_Y = E * N_X H_Y - (E * + \frac{X}{2} E_{N_2} + \frac{Y}{2} E_{H_2})$, where $E(*N_X H_Y)$, $E*$, $E_{N_2}$ and $E_{H_2}$ are the total energies of catalysts with adsorbed species $*N_X H_Y$, clean catalyst surface, free $N_2$, and $H_2$, respectively. $X$ and $Y$ represent the number of nitrogen and hydrogen atoms, respectively.

**Table S3.** Adsorption energy (in eV) of key intermediates *NH-NH, *NH-$NH_2$,

*$NH_2$-$NH_2$, *$NH_2$-$NH_3$ on B@$MSi_2N_4$ for NRR via the alternating mechanism.

| M | $\Delta E_{ads}$ (*NH-NH) | $\Delta E_{ads}$ (*NH-$NH_2$) | $\Delta E_{ads}$ (*$NH_2$-$NH_2$) | $\Delta E_{ads}$ (*$NH_2$-$NH_3$) |
|---|---|---|---|---|
| **Cr** | -2.22 | -2.68 | -3.56 | -4.42 |
| **Hf** | -1.75 | -2.19 | -3.10 | -3.91 |
| **Mo** | -1.90 | -2.33 | -3.23 | -4.27 |
| **Nb** | -1.83 | -2.38 | -3.41 | -4.11 |
| **Ta** | -1.78 | -2.25 | -3.13 | -3.99 |
| **Ti** | -2.01 | -2.47 | -3.36 | -4.19 |
| **V** | -2.08 | -2.53 | -3.42 | -4.25 |
| **W** | -1.94 | -2.41 | -3.38 | -4.31 |
| **Zr** | -1.72 | -2.17 | -3.07 | -3.88 |

**Table S4.** Adsorption energy (in eV) of key intermediates *N-N, *N-NH, *NH-NH,

*NH-$NH_2$, *$NH_2$-$NH_2$, and *$NH_2$-$NH_3$ on B@$MSi_2N_4$ for NRR via enzymatic mechanism.

| M | $\Delta E_{ads}$ (*N-N) | $\Delta E_{ads}$ (*N-NH) | $\Delta E_{ads}$ (*NH-NH) | $\Delta E_{ads}$ (*NH-$NH_2$) | $\Delta E_{ads}$ (*$NH_2$-$NH_2$) | $\Delta E_{ads}$ (*$NH_2$-$NH_3$) |
|---|---|---|---|---|---|---|
| **Cr** | -0.66 | 0.18 | -0.98 | -1.38 | -3.64 | -4.28 |
| **Hf** | -0.26 | 0.65 | -0.54 | -0.96 | -3.21 | -3.76 |
| **Mo** | -0.38 | 0.61 | -0.59 | -1.09 | -3.33 | -3.92 |
| **Nb** | -0.32 | 0.68 | -0.53 | -1.01 | -3.27 | -3.97 |
| **Ta** | -0.29 | 0.83 | -0.53 | -0.7 | -3.25 | -3.84 |
| **Ti** | -0.48 | 0.66 | -0.74 | -1.18 | -3.45 | -4.04 |
| **V** | -0.53 | 0.59 | -0.82 | -1.22 | -3.51 | -4.12 |
| **W** | -0.41 | 0.49 | -0.65 | -1.17 | -3.32 | -4.02 |
| **Zr** | -0.23 | 0.96 | -0.44 | -0.91 | -3.18 | -3.73 |

**Table S5.** Adsorption energy (in eV) of key intermediates *N-N, *N-NH, *N-$NH_2$,

*N-$NH_3$, *NH, *$NH_2$, and *$NH_3$ on $B_2$@$MSi_2N_4$ for NRR via distal mechanism.

| M | $\Delta E_{ads}$ (*N-N) | $\Delta E_{ads}$ (*N-NH) | $\Delta E_{ads}$ (*N-$NH_2$) | $\Delta E_{ads}$ (*N-$NH_3$) | $\Delta E_{ads}$ (*NH) | $\Delta E_{ads}$ (*$NH_2$) | $\Delta E_{ads}$ (*$NH_3$) |
|---|---|---|---|---|---|---|---|
| **Cr** | 0.51 | -0.90 | -1.54 | -1.79 | -1.48 | -2.43 | -2.72 |
| **Hf** | 0.33 | -0.82 | -1.51 | -1.61 | -1.69 | -2.10 | -3.72 |
| **Mo** | -0.16 | -1.41 | -1.87 | -2.19 | -1.99 | -3.12 | -3.83 |
| **Nb** | -0.28 | -1.58 | -2.00 | -2.65 | -2.18 | -3.29 | -3.76 |
| **Ta** | -0.022 | -1.30 | -1.78 | -2.30 | -2.07 | -3.05 | -3.77 |
| **Ti** | 0.071 | -1.27 | -1.77 | -2.37 | -2.06 | -2.83 | -3.27 |
| **V** | 0.13 | -1.22 | -1.70 | -2.34 | -1.59 | -2.59 | -3.02 |
| **W** | -0.29 | -1.55 | -2.17 | -2.28 | -2.15 | -3.19 | -3.89 |
| **Zr** | 0.35 | -0.82 | -1.51 | -1.76 | -1.70 | -2.77 | -3.69 |

**Table S6.** Adsorption energy (in eV) of key intermediates *NH-NH, *NH-$NH_2$,

*$NH_2$-$NH_2$, *$NH_2$-$NH_3$, and *$NH_3$ on $B_2$@$MSi_2N_4$ for NRR via the alternating mechanism.

| M | $\Delta E_{ads}$ (*NH-NH) | $\Delta E_{ads}$ (*NH-$NH_2$) | $\Delta E_{ads}$ (*$NH_2$-$NH_2$) | $\Delta E_{ads}$ (*$NH_2$-$NH_3$) | $\Delta E_{ads}$ (*$NH_3$) |
|---|---|---|---|---|---|
| **Cr** | -0.24 | -2.30 | -2.07 | -3.83 | -2.72 |
| **Hf** | -1.88 | -2.23 | -3.04 | -4.17 | -3.72 |
| **Mo** | -0.80 | -2.79 | -3.15 | -4.53 | -3.83 |
| **Nb** | -0.77 | -3.13 | -3.13 | -4.65 | -3.80 |
| **Ta** | -0.85 | -3.38 | -3.08 | -4.48 | -3.77 |
| **Ti** | -0.53 | -2.86 | -2.70 | -4.55 | -3.20 |
| **V** | -0.79 | -2.82 | -2.38 | -3.99 | -3.02 |
| **W** | -0.93 | -2.92 | -3.26 | -4.60 | -3.88 |
| **Zr** | -0.31 | -2.32 | -3.02 | -4.18 | -3.70 |

**Table S7.** Adsorption energy (in eV) of key intermediates *N-N, *N-NH, *NH-NH,

*NH-$NH_2$, *$NH_2$-$NH_2$, and *$NH_2$-$NH_3$ and *$NH_3$ on $B_2$@$MSi_2N_4$ for NRR via enzymatic mechanism.

| M | $\Delta E_{ads}$ (*N-N) | $\Delta E_{ads}$ (*N-NH) | $\Delta E_{ads}$ (*NH-NH) | $\Delta E_{ads}$ (*NH-$NH_2$) | $\Delta E_{ads}$ (*$NH_2$-$NH_2$) | $\Delta E_{ads}$ (*$NH_2$-$NH_3$) | $\Delta E_{ads}$ (*$NH_3$) |
|---|---|---|---|---|---|---|---|
| **Cr** | -1.25 | -2.16 | -2.88 | -3.19 | -5.90 | -6.30 | -2.48 |
| **Hf** | -1.81 | -2.42 | -3.25 | -3.42 | -6.10 | -6.73 | -3.72 |
| **Mo** | -2.26 | -2.93 | -3.66 | -3.95 | -6.63 | -7.17 | -3.83 |
| **Nb** | -2.13 | -2.94 | -3.62 | -4.40 | -6.43 | -7.32 | -3.80 |
| **Ta** | -2.08 | -2.79 | -3.48 | -3.77 | -6.34 | -7.09 | -3.77 |
| **Ti** | -1.79 | -2.54 | -3.42 | -3.54 | -6.25 | -6.92 | -3.27 |
| **V** | -1.60 | -2.46 | -3.18 | -3.47 | -6.09 | -6.78 | -3.02 |
| **W** | -2.32 | -3.07 | -3.75 | -4.42 | -6.73 | -7.25 | -3.90 |
| **Zr** | -1.80 | -2.41 | -3.22 | -3.32 | -6.05 | -6.73 | -3.69 |

**Table S8.** Free energy corrections: $E_{ZPE}$ and $S$ represent the zero-point energy change and the entropy change of intermediate for eNRR on B@$MSi_2N_4$ by distal (end-on) and enzymatic (side-on) pathway, respectively. Note that $T$ is set to 298.15 K, and all the energies are in *eV*.

| Species | $E_{ZPE}$ *(eV)* | *TS (eV)* | $E_{ZPE}$ *-TS (eV)* |
|---|---|---|---|
| ***N-N(end-on)** | 0.228 | 0.134 | 0.094 |
| ***N-N(side-on)** | 0.161 | 0.0942 | 0.0668 |
| ***N-NH** | 0.492 | 0.105 | 0.387 |
| ***N-NH** | 0.548 | 0.118 | 0.430 |
| ***N-$NH_2$** | 0.852 | 0.126 | 0.726 |
| ***NH-NH** | 0.844 | 0.102 | 0.742 |
| ***N-$NH_3$** | 1.244 | 0.133 | 1.111 |
| ***NH-$NH_2$** | 1.152 | 0.184 | 0.968 |
| ***NH** | 0.339 | 0.0871 | 0.252 |
| ***$NH_2$-$NH_2$** | 1.525 | 0.161 | 1.364 |
| ***$NH_2$** | 0.774 | 0.0447 | 0.695 |
| ***$NH_2$-$NH_3$** | 1.807 | 0.158 | 0.929 |
| ***$NH_3$** | 1.157 | 0.0935 | 1.064 |
| ***$NH_3$** | 1.157 | 0.0935 | 1.064 |

**Table S9.** Free energy corrections: $E_{ZPE}$ and $S$ represent the zero-point energy change and the entropy change of intermediate for eNRR on B@$MSi_2N_4$ by alternating pathway. Note that $T$ is set to 298.15 K, and all the energies are in $eV$.

| Species | $E_{ZPE}$ (eV) | TS (eV) | $E_{ZPE}$ -TS (eV) |
|---|---|---|---|
| ***NH-NH** | 0.886 | 0.189 | 0.697 |
| ***NH-$NH_2$** | 1.183 | 0.176 | 1.007 |
| ***$NH_2$-$NH_2$** | 1.503 | 0.141 | 1.362 |
| ***$NH_2$-$NH_3$** | 1.830 | 0.159 | 1.671 |
| ***$NH_3$** | 1.157 | 0.0935 | 1.064 |

**Table S10.** Free energy corrections: $E_{ZPE}$ and $S$ represent the zero-point energy change and the entropy change of intermediate for eNRR on $B_2@MSi_2N_4$ by distal (end-on) and enzymatic (side-on) pathway, respectively. Note that $T$ is set to 298.15 K, and all the energies are in $eV$.

| Species | $E_{ZPE}$ (eV) | TS (eV) | $E_{ZPE}$ -TS (eV) |
|---|---|---|---|
| ***N-N(end-on)** | 0.257 | 0.0927 | 0.164 |
| ***N-N(side-on)** | 0.249 | 0.0592 | 0.190 |
| ***N-NH** | 0.550 | 0.102 | 0.448 |
| ***N-NH** | 0.585 | 0.0614 | 0.524 |
| ***N-$NH_2$** | 0.864 | 0.0903 | 0.774 |
| ***NH-NH** | 0.909 | 0.0713 | 0.838 |
| ***N-$NH_3$** | 1.200 | 0.103 | 1.097 |
| ***NH-$NH_2$** | 1.230 | 0.0961 | 1.134 |
| ***NH** | 0.414 | 0.0373 | 0.377 |
| ***$NH_2$-$NH_2$** | 1.441 | 0.165 | 1.276 |
| ***$NH_2$** | 0.730 | 0.0798 | 0.650 |
| ***$NH_2$-$NH_3$** | 1.807 | 0.139 | 1.668 |
| ***$NH_3$** | 1.080 | 0.105 | 0.975 |
| ***$NH_3$** | 1.082 | 0.104 | 0.978 |

**Table S11.** Free energy corrections: $E_{ZPE}$ and $S$ represent the zero-point energy change and the entropy change of intermediate for eNRR on $B_2@MSi_2N_4$ by alternating pathway. Note that $T$ is set to 298.15 K, and all the energies are in $eV$.

| Species | $E_{ZPE}$ (eV) | TS (eV) | $E_{ZPE}$ -TS (eV) |
|---|---|---|---|
| ***NH-NH** | 0.853 | 0.119 | 0.694 |
| ***NH-$NH_2$** | 1.188 | 0.181 | 1.104 |
| ***$NH_2$-$NH_2$** | 1.537 | 0.175 | 1.378 |
| ***$NH_2$-$NH_3$** | 1.861 | 0.146 | 1.715 |
| ***$NH_3$** | 1.074 | 0.152 | 0.922 |

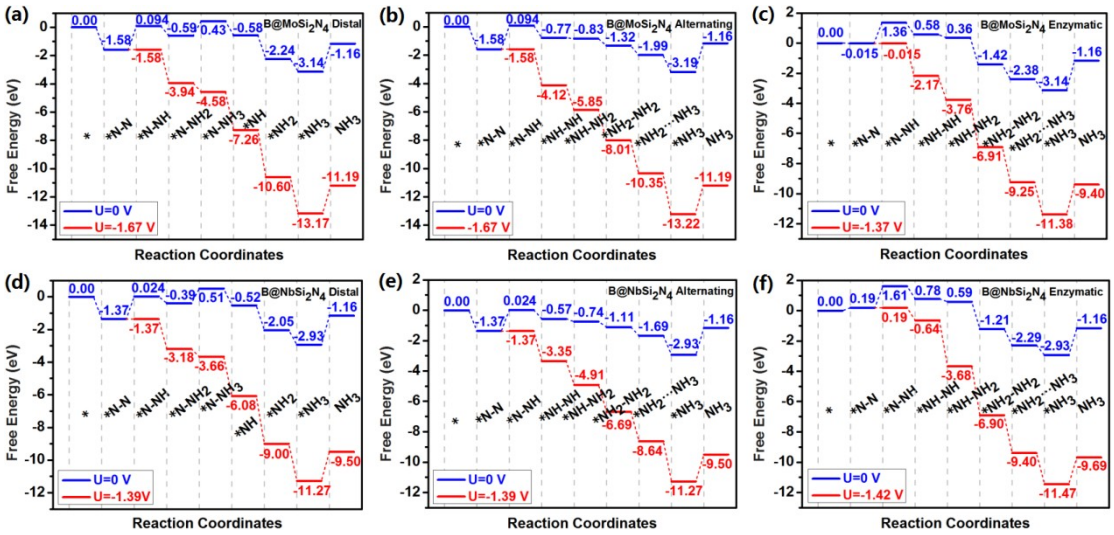


**Fig. S4** Free-energy diagrams of the eNRR on (a-c) B@$MoSi_2N_4$ and (d-f) B@$NbSi_2N_4$ via (a, d) distal, (b, e) alternating, (c, f) enzymatic pathways at 0 V and the limiting potentials.

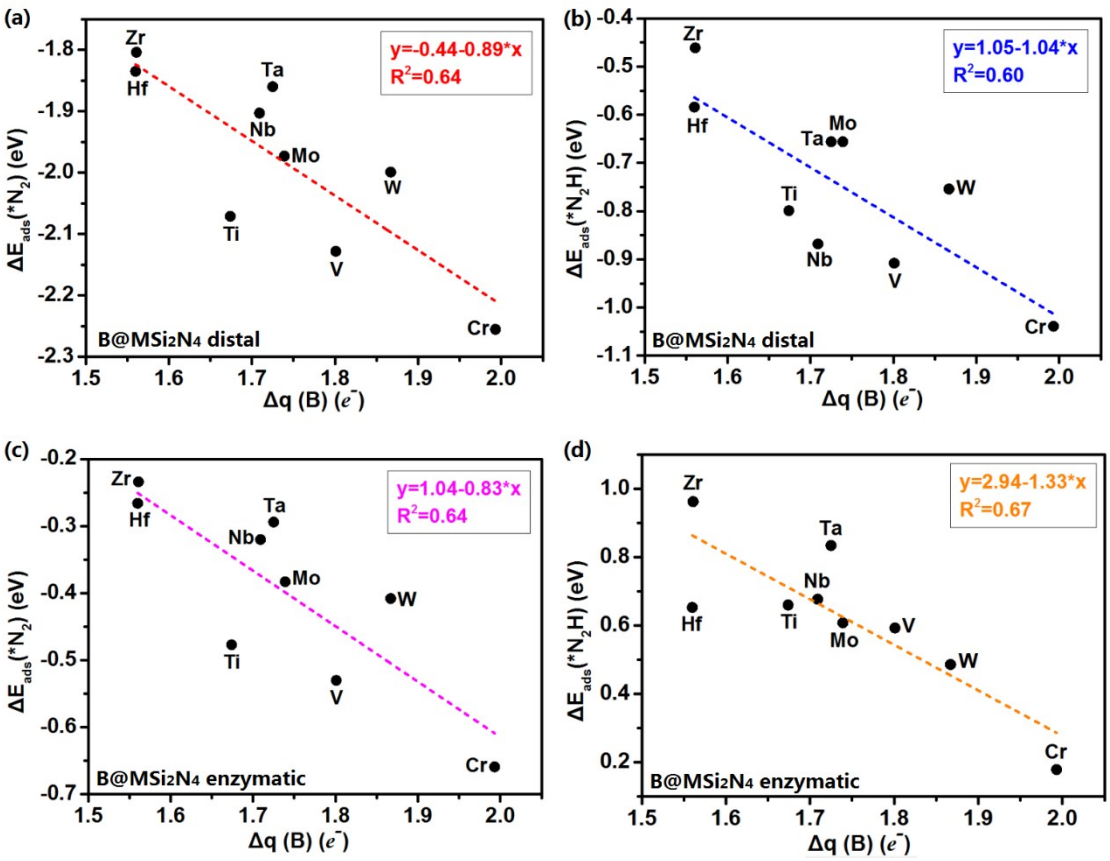


**Fig. S5** Scaling relationship between the polarized charges of B (Δq(B)) and ΔE(*$N_2$) (a, c), and ΔE(*$N_2$H) (b, d) via (a, b) distal and (c, d) enzymatic pathways on B@$MSi_2N_4$.

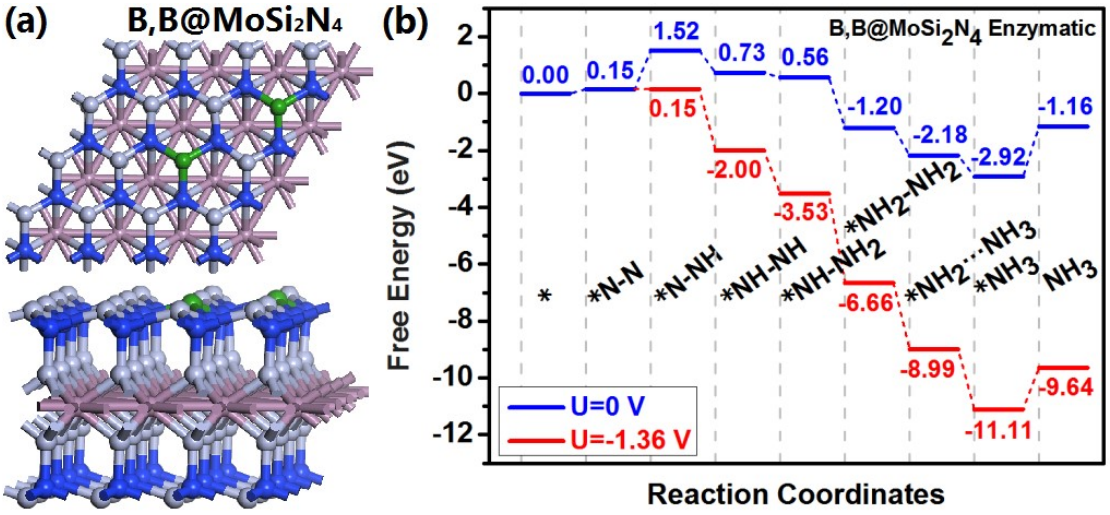


**Fig. S6** (a) Top and side view of schematic structure of B, B@$MoSi_2N_4$ with two non-neighboring B doping. (b) Free-energy diagram of the eNRR on this catalyst via enzymatic pathways at 0 V and the limiting potentials.

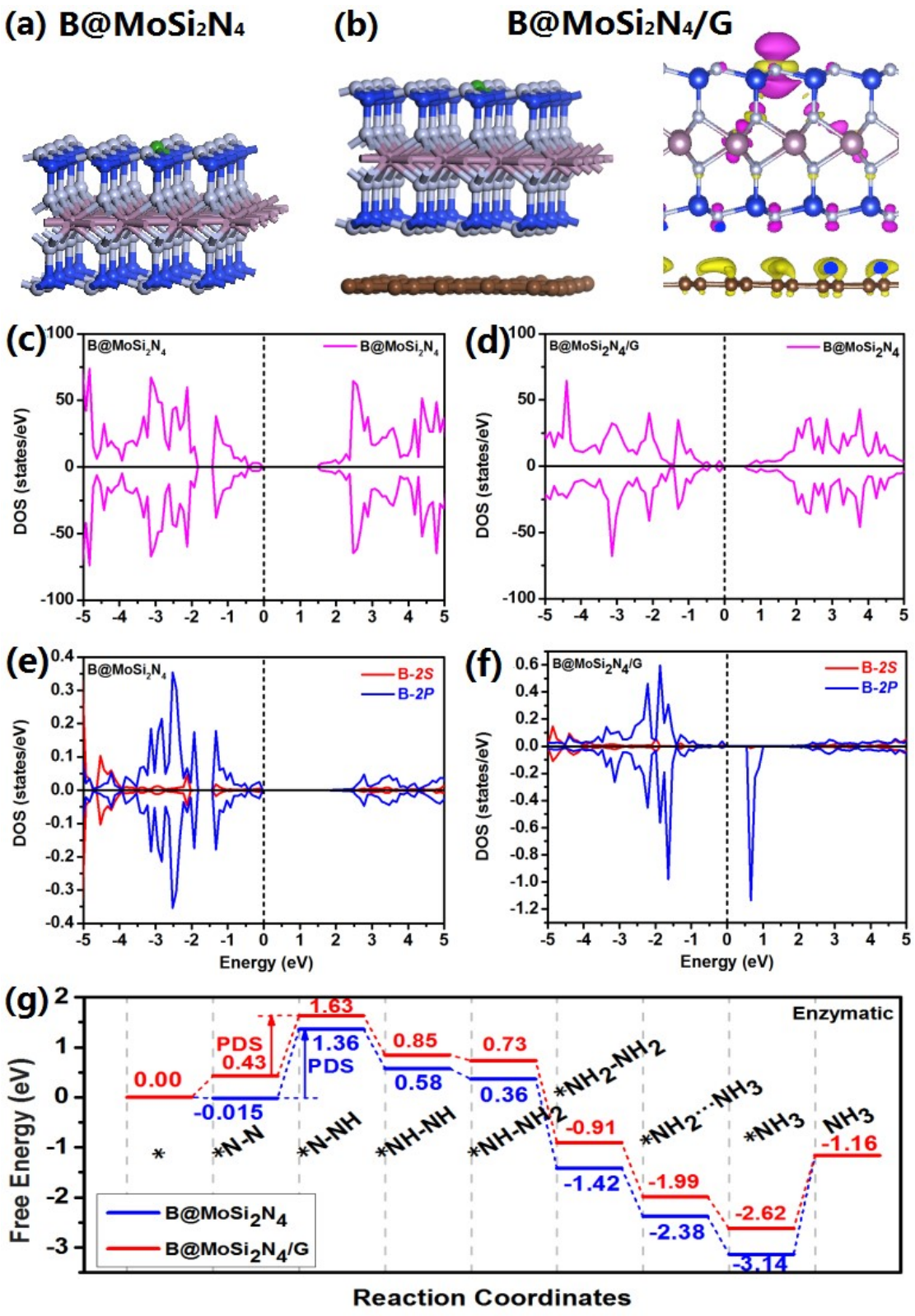


**Fig. S7** (a) Side view of schematic geometrical structures of $B@MoSi_2N_4$. (b) Schematic geometrical structures of $B@MoSi_2N_4$ supported on graphene (namely $B@MoSi_2N_4/G$) (left panel) and corresponding charge density differences (right panel) which are obtained

by subtracting the electronic charges of the B@$MoSi_2N_4$ and graphene from system. The purple and yellow areas define electron accumulation and depletion, respectively. All isosurface values are set to 0.005 *e*/Å$^3$. Density of states (DOS) of (c, d) B@$MoSi_2N_4$ and partial DOS of B atom (e, f) for B@$MoSi_2N_4$ (c, e) without and (d, f) with graphene support. The Fermi level is set to 0. (g) Comparison of free-energy diagrams of NRR catalyzed by B@$MoSi_2N_4$ and B@$MoSi_2N_4$/G via the enzymatic pathway.

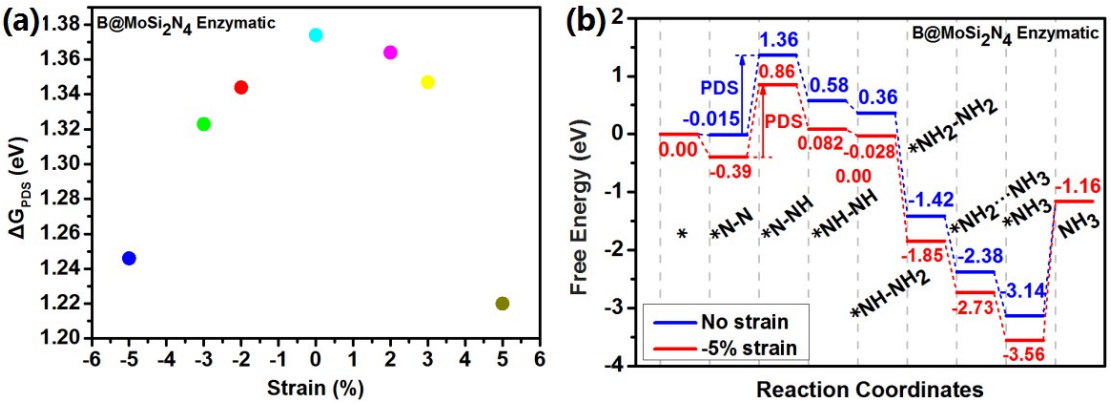


**Fig. S8** (a) Free energy change of the potential-determining step of eNRR on B@$MoSi_2N_4$ by enzymatic pathway as a function of the external strain. (b) Comparison of free-energy diagrams of eNRR catalyzed by B@$MoSi_2N_4$ without strain and with strain of -5% via the enzymatic pathway.

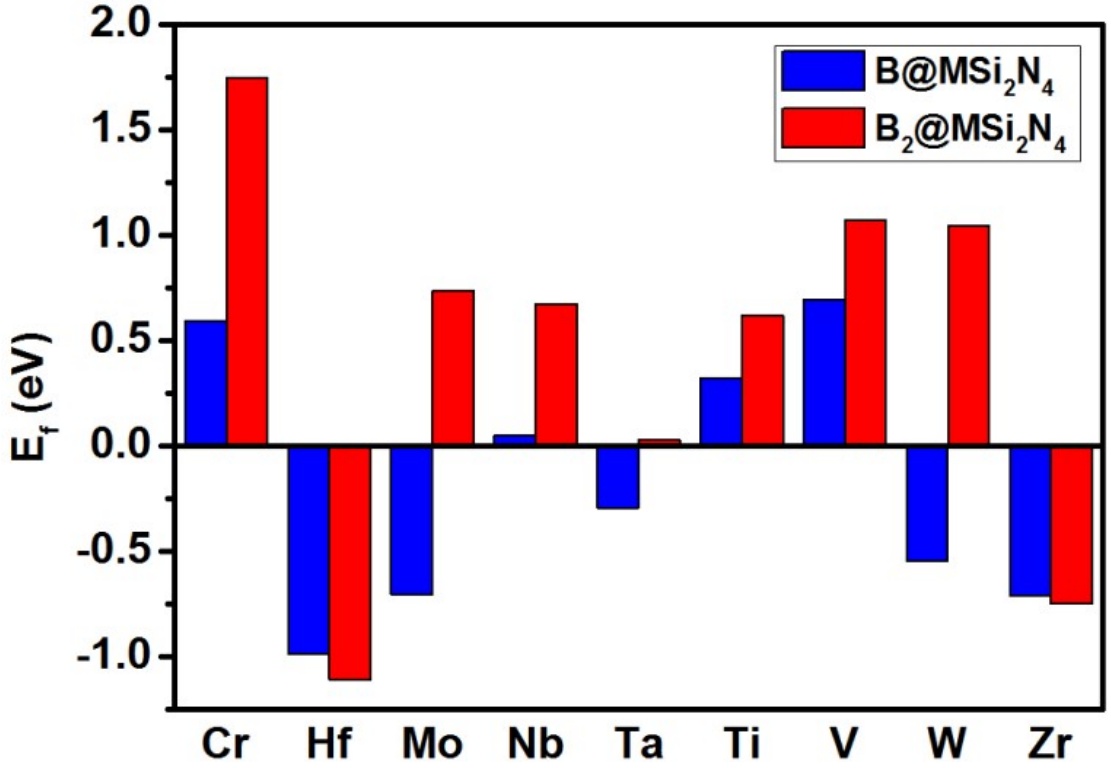


**Fig. S9** Formation energy ($E_f$) of single-B and double B-doped $MSi_2N_4$.